

APPLICATION OF ACOUSTIC IMPEDANCE INVERSION TO PREDICT THE “Y” FIELD RESERVOIR DISTRIBUTION

Eki Komara^{1*}, Desak P. M. E. P¹, Satriana¹, and M. Haris Miftakhul F.¹

¹Geophysics Engineering Department, Faculty of Civil Planning and Geo Engineering, Sepuluh Nopember Institute of Technology
e-mail : komara@its.ac.id

Abstract. Identification of accurate reservoir distribution is necessary to identify prospective and productive zones. One way to identify the distribution of reservoirs in the "Y" field is the inversion method. The inversion method used in this study is acoustic impedance inversion which can be relied upon to characterize the reservoir. This research was conducted to know the best acoustic impedance inversion method and identify the distribution of reservoirs in Field "Y". On research, there are 5 well data and PSTM 3D seismic data. The analytical method used compares the results of cross-section seismic of 3 methods inversion seismic, namely Model-based, Band-Limited, and Sparse spike to get layer prospect hydrocarbons. The goal is to determine the best inversion by identifying the smallest error value. After comparing the results of cross-section seismic and pre-analytical inversion, it has been determined that the Model-Based method is the most effective. This method provides results that support the cross-section and have a small margin of error with a good correlation value. The smallest RMS error value in the method of the model-based inversion is $1944.97 \text{ (ft/s)} * \text{ (g/cc)}$. The reservoir in Field "Y" is identified as sandstone with an impedance value ranging from 24139 to 26722 $\text{(ft/s)} * \text{ (g/cc)}$ and a porosity value of 20 to 23%. It is located at a depth of -935 to -950 m on the Top Bekasap and at a depth of -1067 to -1078 m on the Bottom Bekasap.

Keywords: Acoustic Impedance Inversion; Reservoir; Seismic

INTRODUCTION

The Central Sumatra Basin is one of the Tertiary basins located on the island of Sumatra (Heidrick and Aulia, 1993). Identifying reservoirs accurately is necessary to identify potential and efficient zones in the field. A commonly used technique is known as the inversion method. The most common seismic inversion methods are divided into three types, namely model-based, band-limited, and sparse spikes. The three inversions were then analyzed to determine the type of inversion that best suited the geology of the observed field. The results of the analysis of this inversion method can be a source of information and recommendations for determining the best borehole location. This study uses 5 well data and PSTM 3D seismic data. This research was conducted to know the best acoustic impedance inversion method and identify the distribution of reservoirs in Field "Y".

This research was conducted in the Central Sumatra Basin. More precisely, about 40 km northwest of Duri City, Riau. The forming factors of a hydrocarbon system in the Central Sumatra Basin are grouped into source rocks, reservoir rocks, cap rocks, and traps. Several seismic properties are used for inversion processing such as wavelets, reflection coefficients, acoustic impedance, and synthetic seismograms. Wavelets are waves that have certain amplitude intervals, frequencies, and phases. The reflection coefficient is a value that represents the boundary between two media that have different acoustic impedances. Acoustic impedance is the ability of a rock to pass seismic waves, often also expressed as the impedance value when the rock is exposed to waves in the normal direction (Simm, 2014). Synthetic seismograms are artificial seismic data created based on good data, namely velocity, density, and wavelet logs from seismic data.

The data utilized includes gamma ray, resistivity, sonic, neutron, and density logs. Gamma rays are effective for differentiating layers between permeable and non-permeable. Through resistivity log analysis, it is possible to detect the presence of water in the formation. A sonic log is a record that describes the speed of sound waves transmitted to the formation and the reflections received by the receiver. The neutron log is used to detect the presence of hydrocarbons and calculate porosity. A density log is a type of well log that displays a curve representing the bulk density of the rock in grams per cubic centimeter (Bjorlykke, 2015)

The result of the seismic inversion is in the form of impedance. Therefore, acoustic impedance is a rock property that is affected by depth, lithology type, pressure, porosity, fluid content, and temperature, so that acoustic impedance can be used as a lithology indicator, lithology mapping, hydrocarbon indicator, flow unit mapping to quantitative analysis. When the error value is small, the outcome of the inversion will closely resemble the original state. The inversions used in this research are model-based, band-limited, and sparse spikes. The principle of model-based inversion is to create a geological model and compare it to the original seismic data. Band-limited inversion, also known as inversion recursive, disregards the impact of seismic wavelets and considers a seismic trace as a reflection coefficient gathering that has been filtered by zero-phase wavelets. Seismic trace inverted by itself, the acoustic trace impedance generated is in the same frequency range as the seismic trace. The sparse-spike inversion is performed by assuming that the reflectivity is a small band of reflectivity stored within a larger reflectivity band (Russel, 2006).

METHOD

Data

This study uses some of the input data in the seismic processing. The data includes:

- PSTM 3D Seismic Data which has Inline, Xline, and coordinates.
- 5 Well Log data, check shot and top.

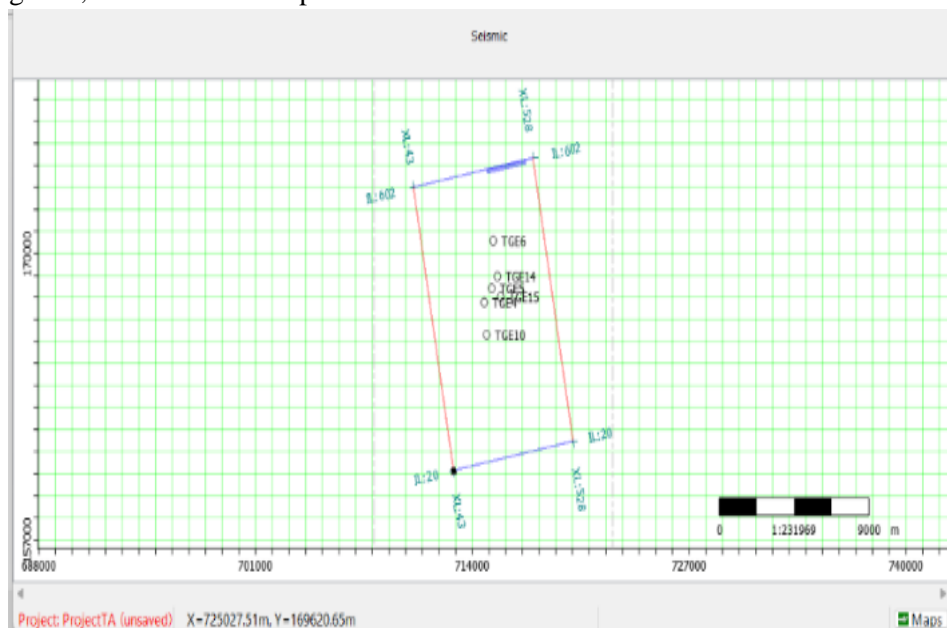


Figure 1 Base map of well and seismic data

Methodology

Data input includes well data which consists of log neutron porosity, gamma ray, density, wave, as well as check shot data. Additionally, post-stack seismic data and well-marker data are also included. The next step involves log analysis, where the gamma-ray log, porosity, and density (NPHI & RHOB) are analyzed to identify potential hydrocarbon prospect zones. The P-wave log's depth domain is converted to a time domain by performing a check shot correction on the data. It can be utilized to accurately position the well in its intended location. Additionally, we performed wavelet extraction using various methods, including the Ricker wavelet method, statistical wavelets, bandpass wavelets, and well-based methods. By inputting wavelength data and the time window range from the prospect zone, wavelet results are obtained.

Additionally, the process of correlating well data and seismic data is done to link well data presented in the depth domain with time domain seismic data. It is important to correlate well data with seismic data to accurately determine the true depth of the seismic horizon. To determine the effectiveness of the correlation

process, examine the current correlation value and time shift. The correlation value ranges between 0 and 1, with a higher value (closer to 1) indicating a stronger correlation. To proceed, choose the horizon through the utilization of the well-seismic tie data. The picking horizon's results serve as a reference for the inversion process. This horizon helps to define the inversion zone. The process of time-to-depth conversion involves transforming seismic data from the time domain to the depth domain. This results in a change from a time structure map to a depth structure map. This process is important because different domains can cause ambiguity when interpreted (Rahman, 2016).

The next step is to make the initial model. To create the initial model, we obtained the volume of acoustic impedance from the log data and picked the horizon by conducting the forward modelling process. In addition, a pre-inversion analysis was conducted to identify the optimal parameters required for performing the inversion process. This analysis was carried out by trial and error to get the parameters, error values, and the best correlation values. Pre-inversion analysis was carried out on the initial model (initial model) using 3 methods that will be compared later, namely Band-Limited, model-based, and Sparse spike by adjusting the parameters to produce a good correlation between the synthetic seismogram and the original seismic and the correlation between the well AI log with inverted AI logs. Seismic inversion is carried out using parameters and methods that have been determined from the pre-inversion analysis process. In this process, reflectivity calculations are carried out to find a suitable acoustic impedance model for further analysis. To identify the distribution of reservoirs in the field, map analysis involved slicing the results of inversion or porosity.

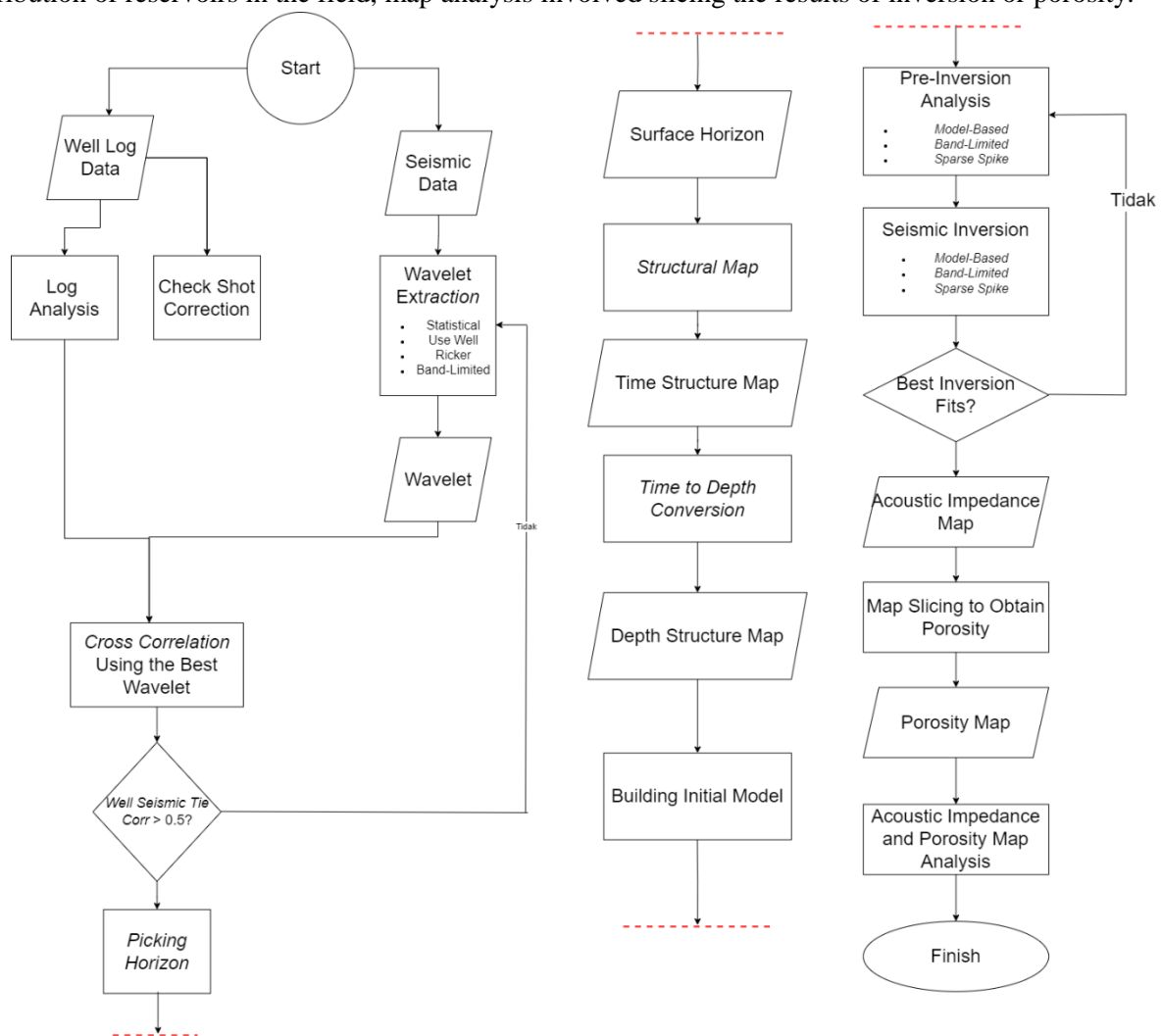


Figure 2 Research flowchart

RESULTS AND DISCUSSION

Log Analysis

This study focuses on the Bekasap Formations. The selection of top and bottom data is done based on existing marker data. Based on the measurement data obtained, the top boundary of the Bekasap Formation in the TGE 6 well is at a depth of 936 m. The top limit of the Bekasap Formation in the TGE 14 well is at a depth of 932 m. The top limit of the Bekasap Formation in the TGE 5 well is at a depth of 922 m. The top limit of the Bekasap Formation in the TGE 15 well is at a depth of 927 m. The top limit of the Bekasap Formation in the TGE 4 well is at a depth of 936 m.

The bottom limit of the Bekasap Formation in the TGE 6 well is at a depth of 1055 m. The bottom limit of the Bekasap Formation in the TGE 14 well is at a depth of 1063 m. The bottom limit of the Bekasap Formation in the TGE 5 well is at a depth of 1052 m. The bottom limit of the Bekasap Formation on the TGE 15 well is at a depth of 1055 m. The bottom limit of the Bekasap Formation in the TGE 4 well is at a depth of 1060 m.

From the results of the data obtained, it was observed that there were zones with low gamma ray values (< 110 API), low-density values, and high porosity values. This zone is assumed to have sandstone lithology because Sandstones have characteristics that are not compact. Whereas zones that have high gamma ray values, high densities, and low porosity can be assumed to be non-sandstone zones which are usually shale stones (Radwan, 2021).

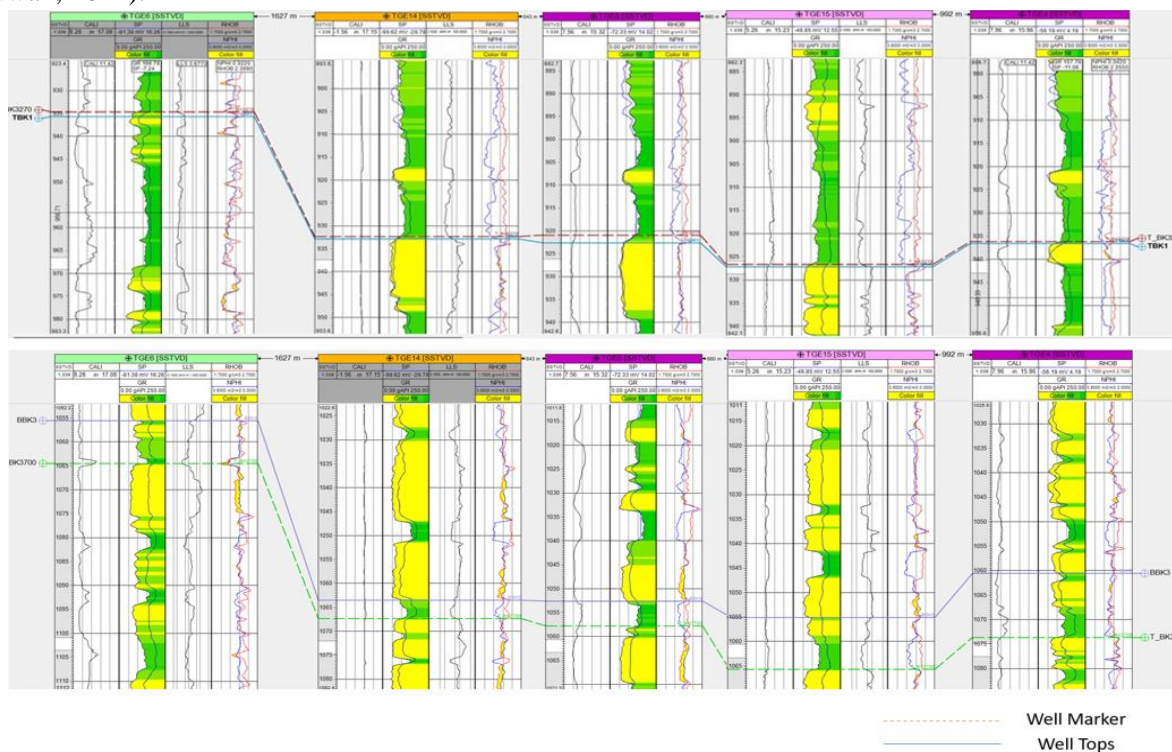


Figure 3 Top (922 m – 936 m) and bottom (1052 m – 1063 m) bekasap log analysis

Well Seismic Tie

Since the correlation value is more than 0.5, it is known that these values are generally good (Santoso, 2006). Furthermore, the well top's conformity to the seismic data can be seen visually. Well seismic tie is appropriate if the well tops of each log fall on a reflector that is continuous with the seismic data.

After doing trial and error, a statistical wavelet has a correlation value of more than 0.5 and the well top falls on a continuous reflector. The trace range adjusts the inline of each well. The trace range used is 400

ms. The taper length used is 25 ms. The wavelet length used in well 4 is 170 ms, in well 5 is 52, in well 6 is 88 ms, in well 14 is 57 ms, and in well 15 is 57 ms.

Table 1 Well seismic tie correlation value

Well	Statistical	Ricker	Bandpass	Use Well
TGE 4	0.538	0.66	0.624	0.582
TGE 5	0.627	0.682	0.707	0.717
TGE 6	0.621	0.654	0.837	0.71
TGE 14	0.739	0.753	0.717	0.677
TGE 15	0.623	0.654	0.645	0.583

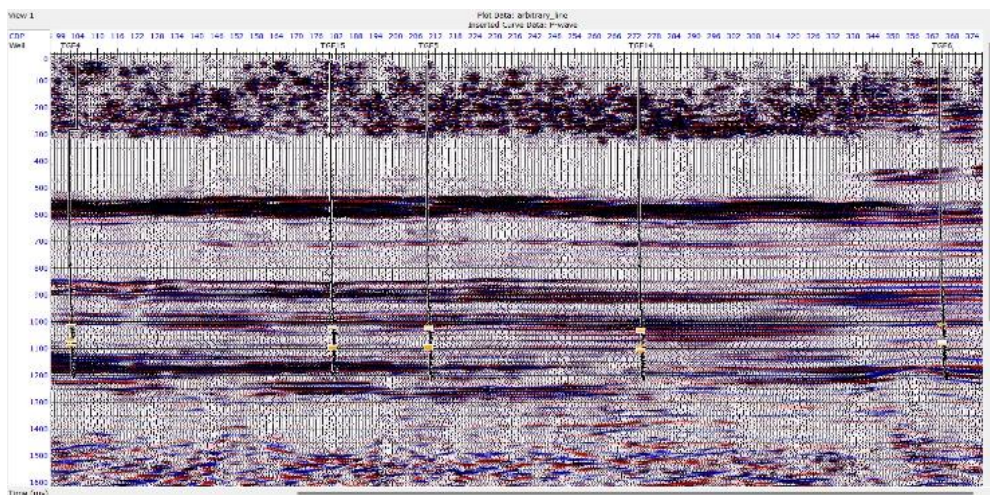


Figure 4 Statistical well seismic tie result on arbitrary line bekasap formation

Cross plot analysis

Cross-plot analysis was carried out to determine the rock lithology zone in the "Y" field. The cross-plot results are sensitive enough to separate the lithology in Field "Y" which is indicated by the cut-off value obtained. The cut-off serves as a boundary between the sandstone zone and the shale zone based on gamma-ray values (Jayadi, 2016). From the results of the cross-plot analysis of well data, there is a correlation between porosity and impedance values. An increase in porosity can cause a decrease in velocity, a decrease in density, and a decrease in acoustic impedance. Zones with high porosity located in the low gamma ray zone are indicated as reservoir zones (Alabi, 2019). Based on the cross-plot results, the porosity value is very good, which is above 21%, so the greater the porosity value, the better the reservoir. The cut-off at the P- Impedance value is 19000 (ft /s) *(g/cc). It can be said that the yellow zone is a sandstone area with good porosity, this is indicated by having low impedance values, high porosity, and low gamma rays. The tight sandstone zone has high impedance and low porosity which is indicated by the red zone. The shale zone has high impedance values and high gamma rays which are shown in blue zones.

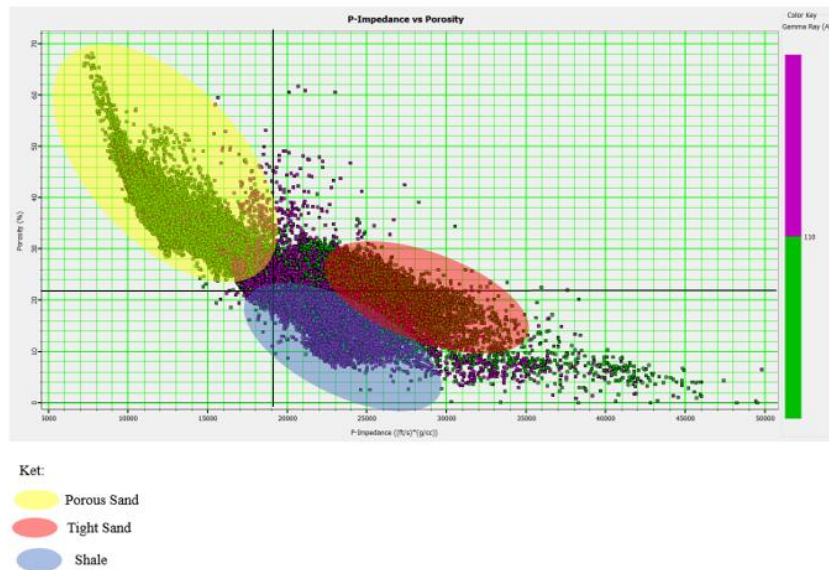


Figure 5 Cross plot p-impedance vs porosity (x-axis: porosity, y-axis: acoustic impedance, color scale: gamma-ray)

Initial Model

Before inversion, the initial model is made as a reference in determining whether the inversion process is good or not. The initial model used in the study namely in the form of impedance P (Z_p). The initial model is created by multiplying the density log with the P-wave in the forward modelling process, which seeks out the seismic synthetic. The initial model was made using a smoother high-cut frequency of 10/15 Hz. The parameters used in this study are as follows:

- Wells: 5 Well logs
- Horizons: Top Bekasap and Bottom Bekasap Horizons
- Wavelets: Statistical Wavelet 14 with wavelength 57

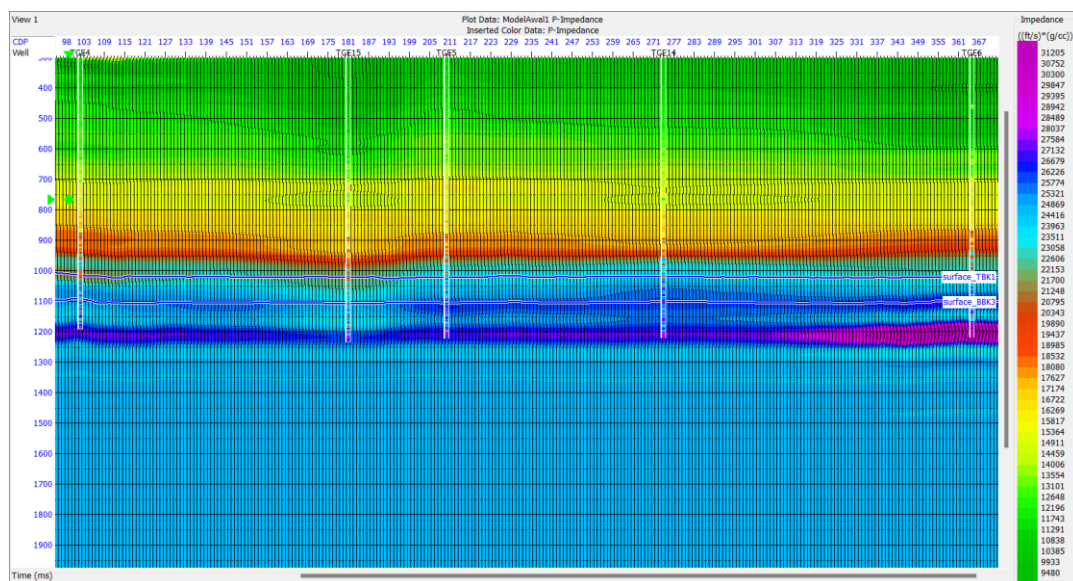


Figure 6 Initial model(5 impedance well logs) on top – bottom bekasap horizon (9480 (ft/s * g/cc) – 31205 (ft/s)*(g/cc))

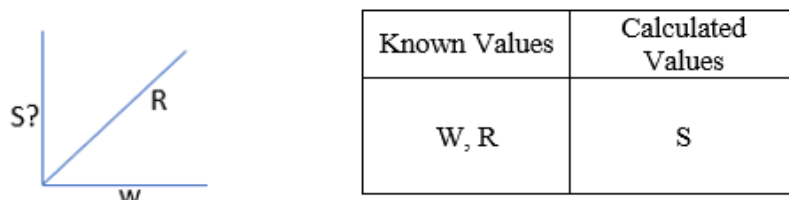


Figure 7 Initial model concept

Inversion Analysis

A sensitivity analysis of the basic model was conducted to obtain more specific information, find the smallest error, and as a guide for the inversion process. Sensitivity analysis was performed on the model-based, sparse spike, and Band Limited inversion. The results are in the form of a curve, where the blue curve represents the well curve, the red curve represents the inversion curve, and the black curve represents the initial model curve. If the three curves coincide, inversion is good. Other results from the sensitivity analysis are error values and correlations. Error-values and correlations are then compared to find out the best inversion method.

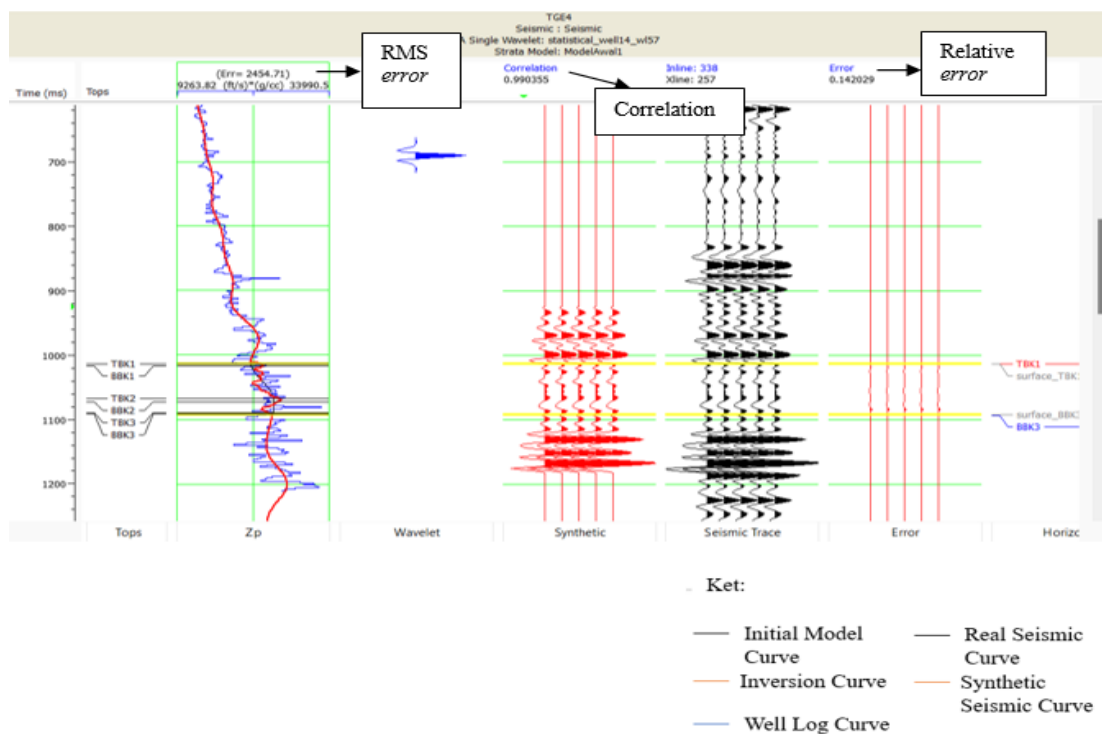


Figure 8 TGE4 log model-based sensitivity analysis

Table 2 RMS error value

Well	Model-based	Band-limited	Linear Sparse Spike
TGE 4	2454.71	2601.21	18589.4
TGE 5	2589.57	2342.42	13063.5
TGE 6	2399.97	2722.53	24720.1

Well	Model-based	Band-limited	Linear Sparse Spike
TGE 14	3107.03	3618.29	31581.5
TGE 15	1944.97	1397.89	8328.68
Map	2524.39	2624.4	20700.4

Table 3 Relative error value

Well	Model-based	Band-limited	Linear Sparse Spike
TGE 4	0.142029	-	0.16066
TGE 5	0.090037	-	0.049319
TGE 6	0.102164	-	0.112
TGE 14	0.053535	-	0.056374
TGE 15	0.069221	-	0.104081
Map	0.142029	-	0.16066

The error value is then calculated to get an error in the form of a decimal or percent using the formula (Maurya, 2020):

Table 4 Inversion error value

Well	Model-based	Band-limited	Linear Sparse Spike
TGE 4	0.1129329	0.11980518	0.855236
TGE 5	0.1191374	0.10788596	0.601008
TGE 6	0.1104145	0.01278233	1.137288
TGE 14	0.142944	0.16664932	1.452958
TGE 15	0.0894815	0.06438329	0.383174
Map	0.1161387	0.12087325	0.952356

Table 5 Inversion correlation value

Well	Model-based	Band-limited	Linear Sparse Spike
TGE 4	2454.71	2601.21	18589.4
TGE 5	2589.57	2342.42	13063.5
TGE 6	2399.97	2722.53	24720.1
TGE 14	3107.03	3618.29	31581.5
TGE 15	1944.97	1397.89	8328.68
Map	2524.39	2624.4	20700.4

Error value in the model-based method shows a smaller value compared to the Band Limited and Sparse methods spikes. The smallest RMS error value for model-based inversion is 1944.97 (ft /s) *(g/cc) and the largest RMS error value is 3107.03 (ft /s) *(g/cc). Based on the results of Kianoush’s (2023) and Karim’s (2016) research which has an RMS error value of 3669.5 (ft /s) *(g/cc) and 4173.83 5 (ft /s) *(g/cc), this error value indicates a good inversion. The RMS error value is then calculated to produce an error value in the form of a percentage. The smallest RMS error value of model-based inversion is 0.0894 or 8.94% and the largest RMS error value of model-based inversion is 0.1429 or 14.29%. The smallest relative error value in the model-based inversion is 0.0535 or 5.35%, while the biggest relative error value in the model-based inversion is 0.1420 or 14.2%. Based on Kianoush’s (2023) research results, the smallest relative error value is 6.61% and the biggest relative error value is 22.1% indicating good inversion results. An error value close to 0 indicates a good inversion result.

The results of the comparison of the inversion correlations show that the overall inversion results have a very good total correlation. The inversion results for all methods correlate values close to one. Based on the results of sensitivity analysis, the Sparse Spike method correlation is better than the Model-based method and Band Limited. However, the correlation results from the Sparse Spike are not supported by good error results, causing the Model-based method to be the best because the error value and correlation support result in a good inversion. From a comparison of the three inversion methods, it can be concluded that the Model-based inversion has better results than the band-limited and Sparse methods spikes.

Model-Based Inversion Results

Therefore, what we are searching for is reflectivity, which is determined by doing an inversion to determine the estimation of the acoustic impedance model that best matches the seismic data. Based on the model-based inversion results, the distribution of acoustic impedance values is in the range of 9476 – 31212 (ft /s) *(g/cc). The inversion results show that the inversion results have a good match with Log AI. The reservoir layer tends to have a lower impedance value than the surrounding shale layers. Low acoustic impedance zones are identified as sandstone layers with the potential for holding hydrocarbons. In the inversion zone, namely the top and bottom Bekasap, a low impedance value is in the range 17627 – 21250 (ft /s) *(g/cc). This reservoir is based on the results of the cross plot, which is in the yellow zone, at a low impedance value, with a green color scale, and has high porosity.

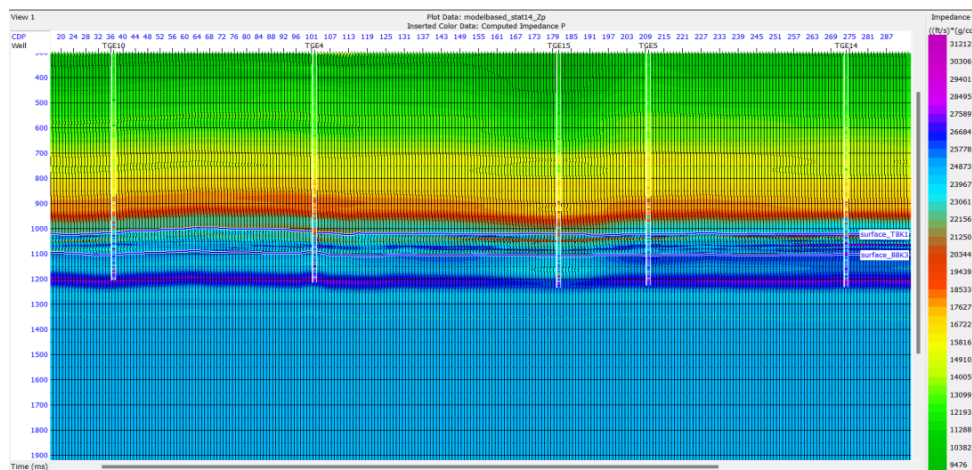


Figure 9 Arbitrary line model-based inversion result (5 impedance well logs) on top – bottom bekasap horizon (9476 (ft/s)*(g/cc) – 31212 (ft/s)*(g/cc))

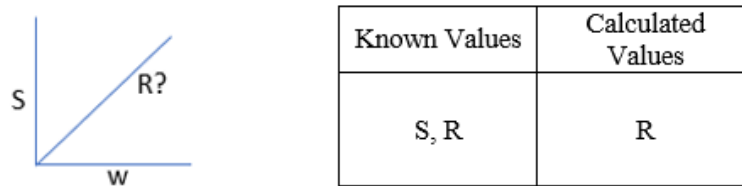


Figure 10 Inversion concept

Porosity

After obtaining the volume of acoustic impedance, the porosity section is made by trace math tools. This is done by obtaining the relationship between the total porosity value and the AI value. Porosity and acoustic impedance are correlated; if the acoustic impedance value is low, the porosity value is high. That correlation was obtained with the cross-plot from both variables. The linear regression function:

$$Y = -0.00145701x + 55.55$$

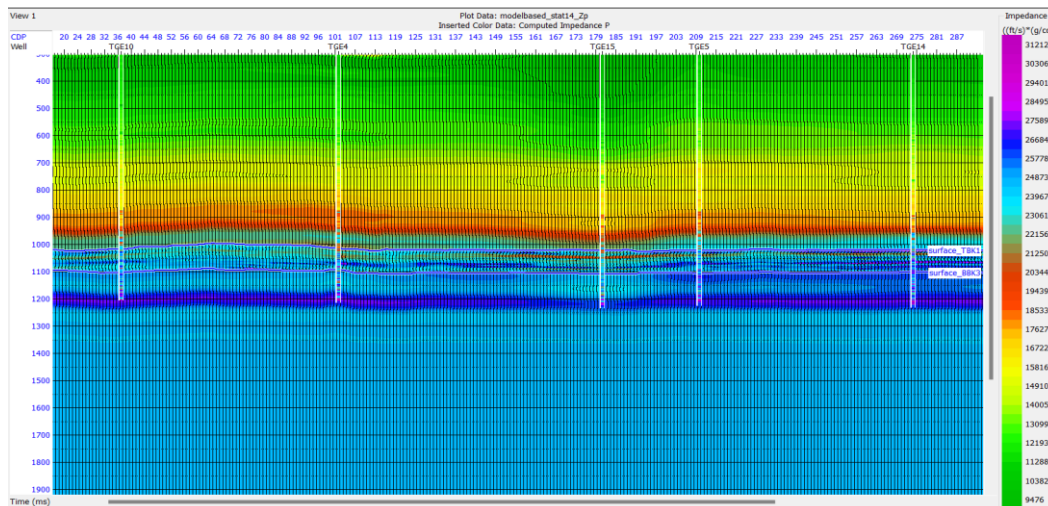


Figure 11 Arbitrary line porosity section result (5 impedance well logs) on top – bottom bekasap horizon (9476 (ft/s) *(g/cc) – 31212 (ft/s) *(g/cc))

A zone with high porosity is marked with a purple zone. The lithology of reservoirs that have a high porosity can be interpreted as sandstone. The results show a porosity value is > 23% where the porosity is considered very good.

Distribution Map

The distribution map of acoustic impedance is made based on the inversion results by doing a slice on the horizon. In the Top Bekasap Slices results, impedance values have a range of 21953 – 24185 (ft/ s) * (g/cc). In the Bottom Bekasap Slices results, impedance values have a range of 24559 – 26722 (ft/ s) * (g/cc).

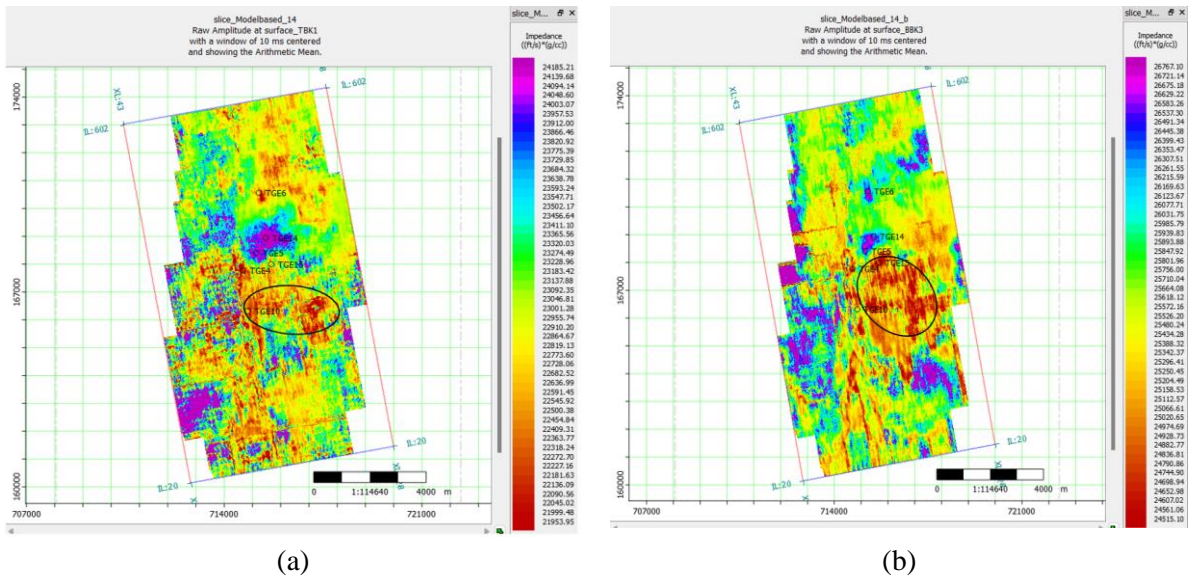


Figure 12 (a) Top bekasap acoustic impedance slice map (x-axis: x coordinate, y-axis: y coordinate, depth 810 ms – 1040 ms) (b) Bottom bekasap acoustic impedance slice map (x-axis: x coordinate, y-axis: y coordinate, depth 930 ms – 1160 ms)

The porosity distribution map is made based on trace math results from porosity that has been done before. This is done by slicing the horizon. In Top Bekasap Slice results, porosity values have a range of 18-23%. In Bottom Bekasap Slice results, porosity values have a range of 16-20 %.

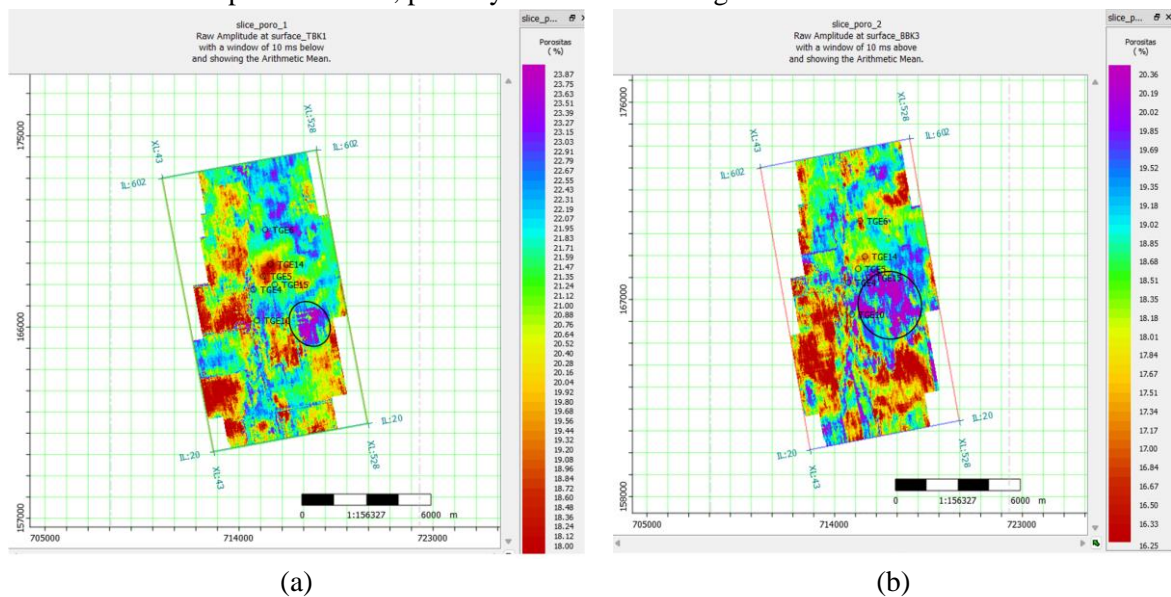


Figure 13 (a) Top bekasap porosity slice map (x-axis: x coordinate, y-axis: y coordinate, depth 810 ms – 1040 ms) (b) Bottom bekasap porosity slice map (x-axis: x coordinate, y-axis: y coordinate, depth 930 ms – 1160 ms)

Based on the results of the inversion and porosity maps on the Top Bekasap (TB) and Bottom Bekasap (BBK) horizons, they are then overlaid to determine reservoir distribution. From the results of the analysis that has been carried out, the relationship between acoustic impedance and porosity states that a porous zone around the TGE 4 and TGE 15 wells has a large porosity (20-23%) and a small acoustic impedance (24139 – 26722 (ft /s) * (g/cc)). This area is recommended for a prospective zone because compared to other areas, this area is an area that has high porosity and low impedance.

Furthermore, a cross-sectional review of the prospective zone was carried out to check the accuracy of the inversion results. It can be seen from the cross-section in the prospective zone area, that the acoustic

impedance appears to be lower, in the range of 16722 – 18533 (ft /s) * (g/cc)). The porosity value in the prospective zone is greater, in the range of 23.51 – 24.17%.

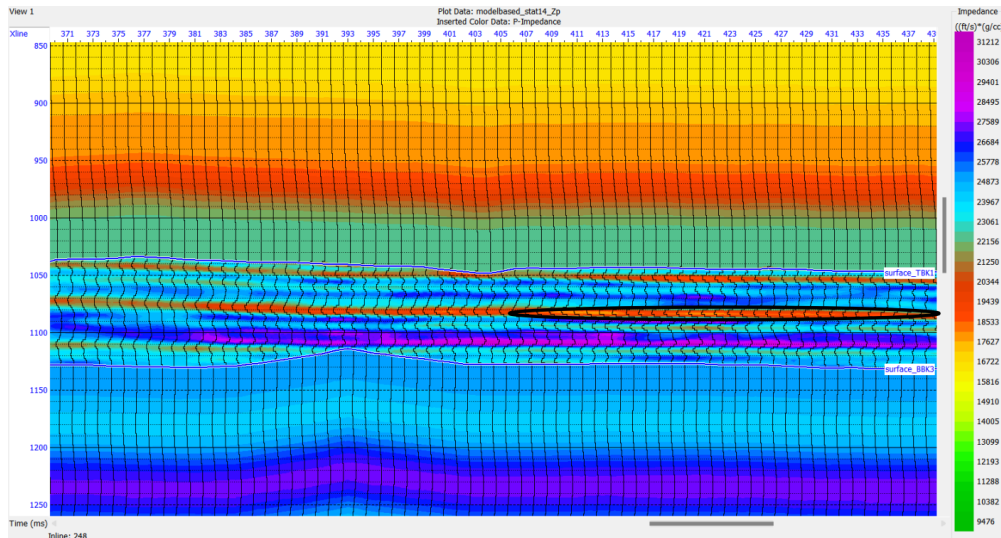


Figure 14 Inversion section of model-based inline 248 in the top – bottom of the bekasap horizon (9476 (ft/s)*(g/cc) – 31212 (ft/s)*(g/cc))

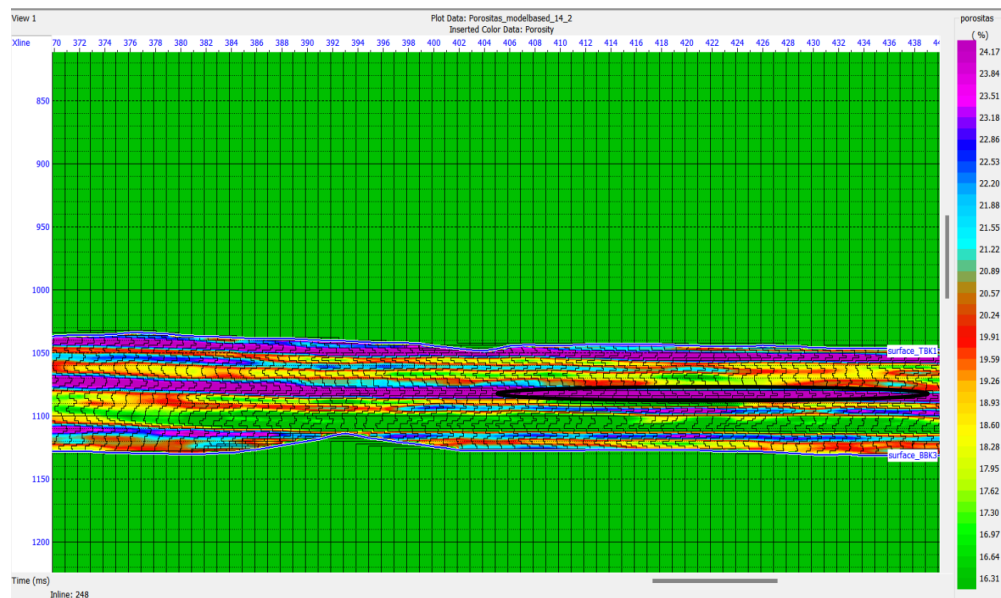


Figure 15 Porosity section of model-based inline 248 in the top – bottom of the bekasap horizon (16.31% - 24.17%)

CONCLUSION

Based on the results of the research analysis that has been carried out, the following conclusions are obtained:

1. The results of the inversion analysis show that model-based is the best inversion in the "Y" Field, where the RMS error value of this method has a range of 1944.97 – 3107.03 (ft /s) * (g/cc) which is smaller than the error value of the band-limited inversion method with a range of 1397.89 – 3618.29 (ft /s) * (g/cc) and sparse spikes 8328.68 – 31581.5 (ft /s) * (g/cc).
2. The distribution of the reservoir in the form of sandstones in Field "Y" is potentially located at UTM coordinates X:716578.48, Y: 166292.95 to X:717888.81, Y:166341.48 for the west to east directions and X:717330.71, Y:166899.58 to X:717354.97, Y: 165249.53 from north to south, from the TBK and BBK horizon with impedance values of 24139 – 26722 (ft/s) * (g/cc), porosity values of 20 – 23 %, and depth values of -935 – -950 m at TBK and depth - 1067 – -1078 m on BBK.

Acknowledgments

The software for processing the data used in this final project are Petrel 2021 and Humpson Russell 10.3.2

REFERENCES

- Alabi, A. &. (2019). Integrating seismic acoustic impedance inversion and attributes for reservoir analysis over 'DJ'Field, Niger Delta. *Journal of Petroleum Exploration and Production Technology*, 9, 2487-2496.
- Bjorlykke, K. (2015). *Petroleum Geoscience: From Sedimentary Environments to Rock Physics*. Springer Science & Business Media.
- Heidrick, T. L., & Aulia, K. (1993). A Structural And Tectonic Model Of The Coastal Plains Block, Central Sumatra Basin, Indonesia.
- Jayadi, H. (2016). Identifikasi Persebaran Litologi Reservoir Batupasir 64 Menggunakan Analisis Seismik Inversi Impedansi Elastik di Lapangan Najlaa Formasi Cibulakan Cekungan Jawa Barat Utara. *Jurnal Fisika: Fisika Sains dan Aplikasinya 1(2)*, 99-106.
- Karim, S. U. (2016). Seismic reservoir characterization using model based post-stack seismic inversion: in case of Fenchuganj gas field, Bangladesh. *Journal of the Japan Petroleum Institute*, 59(6), 283-292.
- Kianoush, P. M. (2023). Inversion of seismic data to modeling the Interval Velocity in an Oilfield of SW Iran. *Results in Geophysical Science*, 13, 100051.
- Maurya, S. P. (2020). *SEISMIC INVERSION METHODS: A PARTICAL APPROACH (VOL. 1)*. Berlin/Heidelberg, Germany : Springer.
- Radwan, A. E. (2021). Modelin the depositional environment of the sandstone reservoir in the Middle Miocene Sidri Member, Badri Field, Gulf of Suez Basin, Egypt: Iteration of gamma-ray log patterns and petrographic characteristics of lithology. *Natural Resource Research* , 431-449.
- Rahman, F. A., Bahri, A. S., & Rochman, J. P. G. N. (2016). Analisis Peta Struktur Domain Kedalaman Dengan Interpretasi Seismik 3d Dalam Studi Pengembangan Lapangan “Kapasida”, Blok “Patala”, Energi Mega Persada Tbk. *Jurnal Geosaintek*, 2(3), 135-144.
- Russel, B. H. (2006). *Introduction to Seismic Inversion Methods (NO.2)*. SEG Books
- Santoso, S. (2006). *SSBBI: Spss Statistik Nonparametrik+ Cd*. Elex Media Komputindo.
- Simm, R. B. (2014). *Seismic Amplitude : An Interpreter's Handbook*. Cambridge University Press.
-